Influence of the Southern Annular Mode on Projected Weakening of the Atlantic Meridional Overturning Circulation

PETER T. SPOONER AND HELEN L. JOHNSON

Department of Earth Sciences, University of Oxford, Oxford, United Kingdom

TIM J. WOOLLINGS

Department of Meteorology, University of Reading, Reading, United Kingdom

(Manuscript received 9 September 2012, in final form 29 April 2013)

ABSTRACT

Coupled climate models predict density-driven weakening of the Atlantic meridional overturning circulation (AMOC) under greenhouse gas forcing, with considerable spread in the response between models. There is also a large spread in the predicted increase of the southern annular mode (SAM) index across these models. Regression analysis across model space using 11 non-eddy-resolving models suggests that up to 35% of the intermodel spread in the AMOC response may be associated with uncertainty in the magnitude of the increase in the SAM. Models with a large, positive SAM index response generally display a smaller weakening of the AMOC under greenhouse gas forcing. The initial AMOC strength is also a major cause of intermodel spread in its response to climate change. The increase in the SAM acts to reduce the weakening of the AMOC over the next century by around 1/3, through increases in wind stress over the Southern Ocean, northward Ekman transport, and upwelling around Antarctica. The SAM response is also related to an increase in the northward salt flux across 30°S and to salinity anomalies in the high-latitude North Atlantic. These provide a positive feedback by further reinforcement of the AMOC. The results suggest that, compared with the real ocean where eddies oppose wind-driven changes in Southern Ocean circulation, climate models underestimate the effects of anthropogenic climate change on the AMOC.

1. Introduction

The Atlantic meridional overturning circulation (AMOC) consists of a northward flux of warm water in the Atlantic basin, which cools and sinks at high latitudes, returning southward as dense water in the deep ocean (Wunsch 2002). Because it transports a large amount of heat northward, it plays an important role in Northern Hemisphere climate (Vellinga and Wood 2002; Knight et al. 2005).

It is generally predicted that the AMOC will weaken in response to anthropogenic climate change (e.g., Thorpe et al. 2001; Gregory et al. 2005; Cheng et al. 2013) with the potential for both regional and global climate impacts, such as moderation of global warming in Europe (Christensen et al. 2007; Meehl et al. 2007). Similar but larger changes in climate have been linked to the AMOC "bipolar seesaw" during glacial periods (Broecker 1998). AMOC strength, estimated using proxies such as $^{231}Pa/^{230}Th$ and ^{14}C (McManus et al. 2004; Robinson et al. 2005), is correlated with Arctic temperature as well as the intensity of Asian monsoons and climate over the Americas; it is thought to be the driver of such changes, although modeling has proved inconclusive (Wang et al. 2001; Alley 2007; Seager and Battisti 2007; Broecker et al. 2010).

A weakening AMOC may also reduce the oceanic capacity for uptake of anthropogenic CO_2 via increases in North Atlantic stratification and the associated weakening of the biological pump and decreased transport of CO_2 to depth (Schmittner 2005; Obata 2007; Zickfeld et al. 2008). The paleoclimate record also hints that changes in AMOC strength are related to the capacity for terrestrial storage of methane and nitrous oxide, two potentially potent greenhouse gases (Flückiger et al. 2004; Sowers 2006; Wolff et al. 2010).

Corresponding author address: Peter Spooner, School of Earth Sciences, University of Bristol, Wills Memorial Building, Queen's Road, Bristol BS8 1RJ, United Kingdom.
E-mail: peter.spooner@earth.oxfordalumni.org

DOI: 10.1175/JCLI-D-12-00663.1

These physical and chemical factors make it important to understand how the AMOC is likely to vary in the near future; however, climate models differ significantly in the magnitude of their simulated AMOC and its response to climate change (Fig. 1). It is necessary to understand why this is the case if the global impacts of a changing AMOC are to be predicted with any skill.

Studies of the response of the AMOC to anthropogenic climate change have mainly been concerned with the effect of density fluxes and meridional steric height gradient in the North Atlantic (e.g., Mikolajewicz and Voss 2000; Thorpe et al. 2001; Gregory et al. 2005). However, numerous modeling studies have found that an increase in the strength of westerly winds over the Southern Ocean can result in an increase in the strength of the AMOC; this is through increased northward Ekman transport, Southern Ocean upwelling and deepening of the Atlantic pycnocline and/or via atmospheric processes (Toggweiler and Samuels 1995; Gnanadesikan 1999; de Boer and Nof 2005; de Boer et al. 2008; Delworth and Zeng 2008; Sijp and England 2009; Klinger and Cruz 2009; Marini et al. 2011; Wolfe and Cessi 2011). The relative contribution of the wind is uncertain (Kuhlbrodt et al. 2007), but it has the potential to affect the sensitivity of the AMOC to climate change.

A useful measure of the strength and location of these westerly winds is the southern annular mode (SAM), the leading mode of atmospheric variability in the Southern Hemisphere (Gong and Wang 1999). It is described by the SAM index, often calculated from the difference in sea level pressure between subpolar and subtropical latitudes. Observational studies have shown a positive trend in the SAM index over the last few decades (Marshall 2003; Jones and Widmann 2004). Modeling studies also consistently predict a similar trend for the twenty-first century (Fig. 1), with a poleward shift and intensification of the Southern Hemisphere jet and a shift in storm tracks (Yin 2005; Fyfe and Saenko 2006). These trends are thought to be due to increases in atmospheric greenhouse gas concentrations and ozone depletion over Antarctica, which both act to increase temperature gradients in the upper troposphere and lower stratosphere, although the mechanisms are not fully understood (Shindell and Schmidt 2004; Toggweiler and Russell 2008; Son et al. 2009). There is some debate as to which effect dominates and which will have the more impact as ozone recovery progresses during this century; changes in ozone are thought to be particularly important during the austral summer and less important in the other seasons because of its strong seasonality (Marshall et al. 2004; Shindell and Schmidt 2004; Perlwitz et al. 2008; Son et al. 2008).

From a modeling perspective, these trends in the SAM might be expected to reinforce the AMOC via the mechanisms outlined above; they have the potential to reduce the impact of anthropogenic forcing on this important part of the climate system. However, these mechanisms are based on non-eddy-resolving models. The real Southern Ocean may be close to an eddy-saturated regime (e.g., Meredith and Hogg 2006), such that an increase in wind strength leads to an increase in southward eddy fluxes, which compensate for the increased northward Ekman transport (Farneti and Delworth 2010). If the SAM is found to reinforce the AMOC in the climate models commonly used for prediction, it may be that the degree of AMOC weakening expected due to climate change is being underestimated.

To test these hypotheses, we carry out an investigation similar to Woollings et al. (2012), who found that the response of the Northern Hemisphere storm track to climate change could be related to the response of the AMOC. We invert their method, which consists of regressions across model space, to discover whether changes in the AMOC are related to changes in the Southern Hemisphere winds.

2. Methods

The discrepancy between different models' predictions of climate is generally used to give an idea of the uncertainty in those predictions. The multimodel regression analysis used here is designed instead to take advantage of this spread in model results, by testing whether the models differ in a systematic way.

We use outputs from the model simulations run for phase 3 of the Coupled Model Intercomparison Project (CMIP3), archived at the Program for Climate Model Diagnosis and Intercomparison (PCMDI). Out of the total 23 models, we use up to 11 of the 12 that include the AMOC streamfunction in the readily available outputs (Table 1). We exclude the Institute of Atmospheric Physics (IAP) Flexible Global Ocean–Atmosphere–Land System Model, gridpoint version 1.0 (FGOALS-g1.0), because its mean overturning circulation for the period 1960–99 is extremely weak and in the opposite direction to the other models. Each model has a different number of ensemble members and therefore, for consistency, only the first ensemble member of each model run is considered.

These models are not able to resolve mesoscale ocean eddies; this may affect the applicability of the results to the real ocean because the Southern Ocean is thought to be eddy saturated (e.g., Meredith and Hogg 2006; Munday et al. 2013). Nevertheless, at present, models of this type are routinely used for comprehensive climate prediction, and it is therefore essential to understand their dynamics.

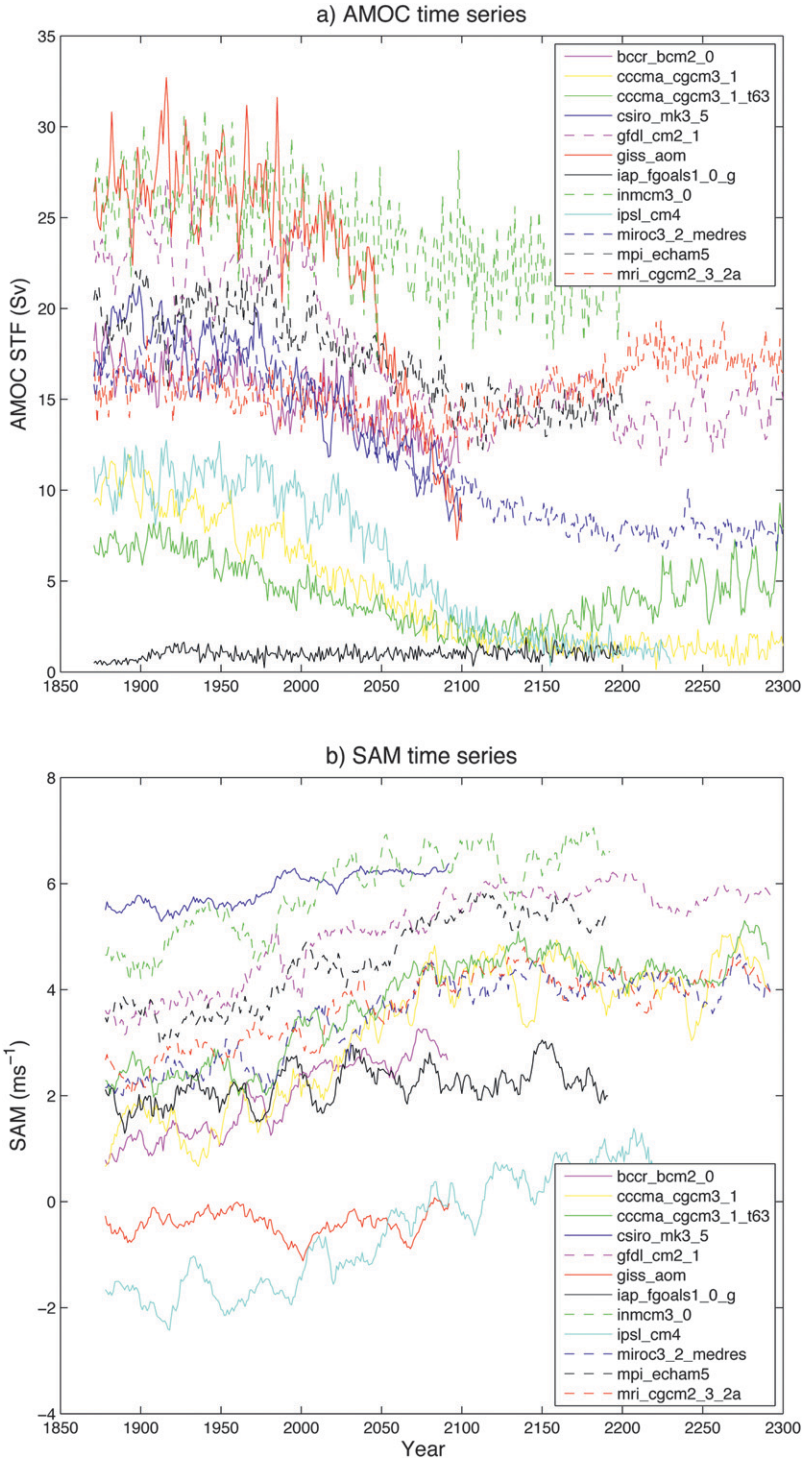

FIG. 1. Modeled evolution of (a) the maximum AMOC streamfunction at 44°N and deeper than 400 m and (b) the 15-yr moving average of the SAM index, defined here as the SAM_{wind} index given in section 2a. The large spread in SAM index values is due to the different latitudinal extent of the band of westerlies vs the band of easterlies in the Southern Hemisphere. The time series are plotted from 1871 to 2100 for all 12 models considered in this study. The name of each model is indicated in the legend. The 20C3M simulations are used for 1850–1999, and the SRES A1B projections are used after this.

TABLE 1. Selected model features of the 11 models used in the analysis, including the original ocean and atmosphere resolution and equilibrium and transient climate sensitivities. We have also included a list of the parameters missing from the available outputs of each model. The identifiers in the final column indicate whether the model includes (Y) or does not include (N) time-varying stratospheric ozone in the twenty-first century. Resolutions and sensitivities were taken from the 2007 International Panel on Climate Change (IPCC) Working Group 1 (WG1) report (Solomon et al. 2007), and details of ozone prescription are from Son et al. (2008, 2009).

Model	Model expansion	Ocean resolution (°lat × °lon)	Atmosphere resolution (°lat × °lon)	Equilibrium climate sensitivity (°C)	Transient climate sensitivity (°C)	Missing parameters	Time-varying ozone
BCCR-BCM2.0	Bjerknes Centre for Climate Research Bergen Climate Model, version 2.0	0.5–1.5 × 1.5	1.9 × 1.9	—	—		N
CGCM3.1(T47)	Canadian Centre for Climate Modelling and Analysis (CCCma) Coupled Global Climate Model, version 3.1 (T47 resolution)	1.9 × 1.9	2.8 × 2.8	3.4	1.9		N
CGCM3.1(T63)	Canadian Centre for Climate Modelling and Analysis (CCCma) Coupled Global Climate Model, version 3.1 (T63 resolution)	0.9 × 1.4	1.9 × 1.9	3.4	—		N
CSIRO Mk3.0	Commonwealth Scientific and Industrial Research Organisation Mark, version 3.0	0.8 × 1.9	1.9 × 1.9	3.1	1.4		Y
ECHAM/MPI-OM	ECHAM/Max Planck Institute Ocean Model	1.5 × 1.5	1.9 × 1.9	3.4	2.2		Y
GFDL CM2.1	Geophysical Fluid Dynamics Laboratory Climate Model, version 2.1	0.3–1.0 × 1.0	2.0 × 2.5	3.4	1.5		Y
GISS-AOM	Goddard Institute for Space Studies, Atmosphere–Ocean Model	3.0 × 4.0	3.0 × 4.0	—	—	barotropic streamfunction	N
INM-CM3.0	Institute of Numerical Mathematics Coupled Model, version 3.0	2.0 × 2.5	4.0 × 5.0	2.1	1.6	potential density, salinity, potential temperature	N
IPSL-CM4	L'Institut Pierre-Simon Laplace Coupled Model, version 4	2.0 × 2.0	2.5 × 3.75	4.4	2.1	potential density	N
MIROC3.2(medres)	Model for Interdisciplinary Research on Climate, version 3.2 (medium resolution)	0.5–1.4 × 1.4	2.8 × 2.8	4.0	2.1		Y
MRI-CGCM 2.3.2	Meteorological Research Institute Coupled Atmosphere–Ocean General Circulation Model, version 2.3.2	0.5–2.0 × 2.5	2.8 × 2.8	3.2	2.2	potential density	N

Annual mean data from the ''twentieth-century climate in coupled models'' (20C3M) scenario was used to generate 1960–99 mean values for a number of different variables (salinity, potential temperature, etc.) at each grid point (longitude, latitude, and depth beneath ocean surface). The 2060–99 means were found using outputs from the Special Report on Emissions (SRES) scenario A1B. Initial conditions for this scenario are determined by the 20C3M results, and CO_2 is then increased approximately linearly to 720 ppm by 2100, after which it is held constant (Solomon et al. 2007).

We define a climate change response in each variable at each grid point as the difference between the 2060–99 and 1960–99 values. We do not extend the study beyond 2099 because not all models have outputs extending into the twenty-second century. The 40-yr length of each time period should ensure a representative value of the state of each variable.

All variables are regridded to a 2° latitude × 2° longitude grid to allow regression analyses across model space at each grid point. Oceanic variables are also regridded to 33 specific and unevenly spaced depth levels below the ocean surface. The regridding process should not significantly influence the results, since we are looking at broad patterns and values, rather than at individual grid points.

a. Climate indices

Here we define indices that represent different modes of climate variability, which will be used as the independent variables in the regression analyses.

A simple SAM index is based on sea level pressure (SLP) (Gong and Wang 1999; Marshall 2003). It is the difference in zonal mean SLP between 40° and 65°S,

$$\mathrm{SAM}_{\mathrm{pressure}} = \overline{\mathrm{SLP}}_{40\mathrm{S}} - \overline{\mathrm{SLP}}_{65\mathrm{S}}.$$

Based on Fig. 1 of Thompson and Wallace (2000), which demonstrates that changes in SLP over the Southern Ocean are well correlated with changes in wind strength, we define a second index,

$$\mathrm{SAM}_{\mathrm{wind}} = \overline{U}_{45\mathrm{S}-70\mathrm{S}} - \overline{U}_{20\mathrm{S}-45\mathrm{S}},$$

where $\overline{U}_{\mathrm{Latitude1-Latitude2}}$ is the mean of the zonal wind velocity between latitudes 1 and 2. For both SAM indices, we use the 40-yr means (described above) of the austral summer months only: December–February (DJF) In recent observational records and in models, the tropospheric SAM signature has shown the largest trends in the austral summer period (Miller et al. 2006), which may be due to coupling between the troposphere and lower stratosphere (Thompson and Solomon 2002; Gillett and Thompson 2003). It is interesting to note that we find that the annual mean AMOC response is more highly correlated with the $\mathrm{SAM}_{\mathrm{djf}}$ index response than with any other season. However, our results are robust if the regressions are carried out using the SAM index calculated for the whole year instead, since the response of the annual mean index is well correlated with the $\mathrm{SAM}_{\mathrm{djf}}$ response in these models.

The response of the $\mathrm{SAM}_{\mathrm{wind}}$ index is dominated by an increase in westerly wind strength between 45° and 70°S and is highly correlated with changes in the $\mathrm{SAM}_{\mathrm{pressure}}$ index with $R^2 = 0.92$ and $p = 2.8 \times 10^{-6}$. We use the $\mathrm{SAM}_{\mathrm{wind}}$ index in the following regression analysis and from here on simply refer to this as the SAM index.

It is thought that ozone depletion should enhance the positive trends in the SAM index, while ozone recovery during the twenty-first century should oppose any increase in the SAM index (Perlwitz et al. 2008; Son et al. 2008). Comparing those models that include time-varying ozone with those that do not indicates that the SAM indices do not show consistently high or low responses when time-varying stratospheric ozone is included. This may be due to the particular set of models or choice of time periods used here. Either way, we conclude that the presence or absence of time-varying stratospheric ozone is not a major factor in our results.

The AMOC index we use is the maximum value of the annual mean AMOC streamfunction at 44°N and below 400 m to avoid surface maxima. This was chosen to be consistent with the study of Woollings et al. (2012).

The North Atlantic Oscillation (NAO) is the dominant mode of climate variability in the North Atlantic sector. A simple NAO index is the pressure difference between Iceland and the Azores (Hurrell and Deser 2009),

$$\mathrm{NAO} = \mathrm{SLP}_{\mathrm{Azores}} - \mathrm{SLP}_{\mathrm{Iceland}}.$$

To avoid unrepresentative, localized anomalies, area mean rather than point values of SLP are used [Iceland = (54°–60°N, 18°–42°W) and Azores = (26°–36°N, 18°–42°W)]. As with the SAM, we use the $\mathrm{NAO}_{\mathrm{djf}}$ index since the largest amplitude trends in SLP occur during the boreal winter months (Miller et al. 2006; Hurrell and Deser 2009).

b. Regression

Every model displays a different response to anthropogenic forcing (2060–99 minus 1960–99) in its climate indices. At each grid point (longitude, latitude, depth), every model has a slightly different response in any given climate variable. If these different climate variable responses are plotted against the different

responses of a climate index, a line of best fit can be drawn. The accompanying statistics describe how closely the response of the climate variable is related to the response of the climate index across model space. Here we carry out the equivalent operation by calculating a linear regression of the response in any given variable across model space on a vector comprising the normalized (to one standard deviation) response of a climate index for each model, as in Woollings et al. (2012) and similar to the methods of other authors (e.g., Hall and Qu 2006; Son et al. 2008). The gradient of the best-fit regression line B is the change in the variable response per one standard deviation of the intermodel spread in the index response. The mean SAM response across the 11 models is 1.56 times larger than the standard deviation of this response; values of B should be scaled accordingly to allow comparisons of the magnitude of the SAM-related response of each variable with the multimodel mean response. A positive value of B suggests that models with the most positive index response also have the most positive response in the climate variable under consideration.

For some variables there are fewer than 11 models with available data (Table 1). When this is the case, the regression is carried out using the maximum number of models possible. Regressions are only carried out at grid points where every model used in that regression analysis has data.

The R^2 statistic is a measure of the proportion of the spread in the data that may be accounted for by the statistical model. The R^2 is calculated for every regression. By the nature of the method, some grid points will have high R^2 values by chance. The R^2 values are therefore only interpreted quantitatively when maps of R^2 show consistent values over a large area or when patterns of R^2 are similar to those of B.

Further statistical analyses are difficult due to the low number of models. The models and the climate indices are not strictly independent, so there is some uncertainty about the number of degrees of freedom compared to the number of models (Pennell and Reichler 2011). Estimates of the p value are included, but these—as well as the estimates of explained variance from R^2—may be overly confident. Values of B are often assumed to be statistically significant when $p < 0.05$, and white contours in maps of B (e.g., section 3) enclose areas where $p < 0.05$.

It is of course possible that regression relationships between two variables do not reflect a direct link but rather an indirect one in which both variables are related to some third factor. In particular, slight differences in model physics such as ocean diffusivity may lead to two unrelated variables each having a particular response. However, since we generally regress oceanic variables on atmospheric climate indices (i.e., spanning two different components of the models), we consider it unlikely that the relationships we find are due to model formulation in this way.

3. Results

a. AMOC–SAM relationship

The multimodel mean, 1960–99 AMOC streamfunction (Fig. 2a) shows water flowing north above 1100 m, with southward-flowing North Atlantic Deep Water (NADW) below. The multimodel mean response of the AMOC to climate change (Fig. 2b) shows a maximum weakening of the AMOC of around 6 Sv ($1\,\mathrm{Sv} \equiv 10^6\,\mathrm{m^3\,s^{-1}}$). The position of maximum weakening is deeper than the maximum of the twentieth century AMOC, suggesting that the models predict both a weakening and shallowing of the AMOC.

Figure 2c shows the regression of the AMOC streamfunction response on the response of the SAM. The coefficient B is positive almost everywhere showing that models with a large positive SAM response generally display a smaller weakening of the AMOC under greenhouse gas forcing. The scaled magnitude of the AMOC pattern associated with the SAM is opposite in sign and around ½ of the mean AMOC response. If causal, this relationship suggests that an increase in the SAM acts to significantly reinforce the AMOC under climate change, reducing the maximum weakening by $\sim$⅓. The significant R^2 values below 1000 m (Fig. 2d) suggest that intermodel spread in the SAM index response can potentially explain up to 35% of the intermodel spread in the middepth AMOC response, although this could be an overestimate (see section 2b).

We also regress the AMOC streamfunction response (across model space) onto a vector comprising the $1960–99_{\mathrm{mean}}$ AMOC index (Fig. 2e). The negative sign of the regression coefficient B shows that models with the greatest initial AMOC index show the greatest reduction in the AMOC streamfunction, consistent with Gregory et al. (2005). The map of R^2 (Fig. 2f) shows that 40%–75% of the intermodel spread in AMOC response in the deep ocean is associated with the initial strength of the AMOC. Clearly, the different initial strengths of the AMOC in each model are important in determining its response to anthropogenic forcing but cannot explain all of the spread. The relationship with the SAM has the potential to explain a large proportion of the remaining spread.

This reinforcement of the AMOC by the SAM is consistent with other non-eddy-resolving studies (e.g., Gnanadesikan 1999; Delworth and Zeng 2008; Klinger

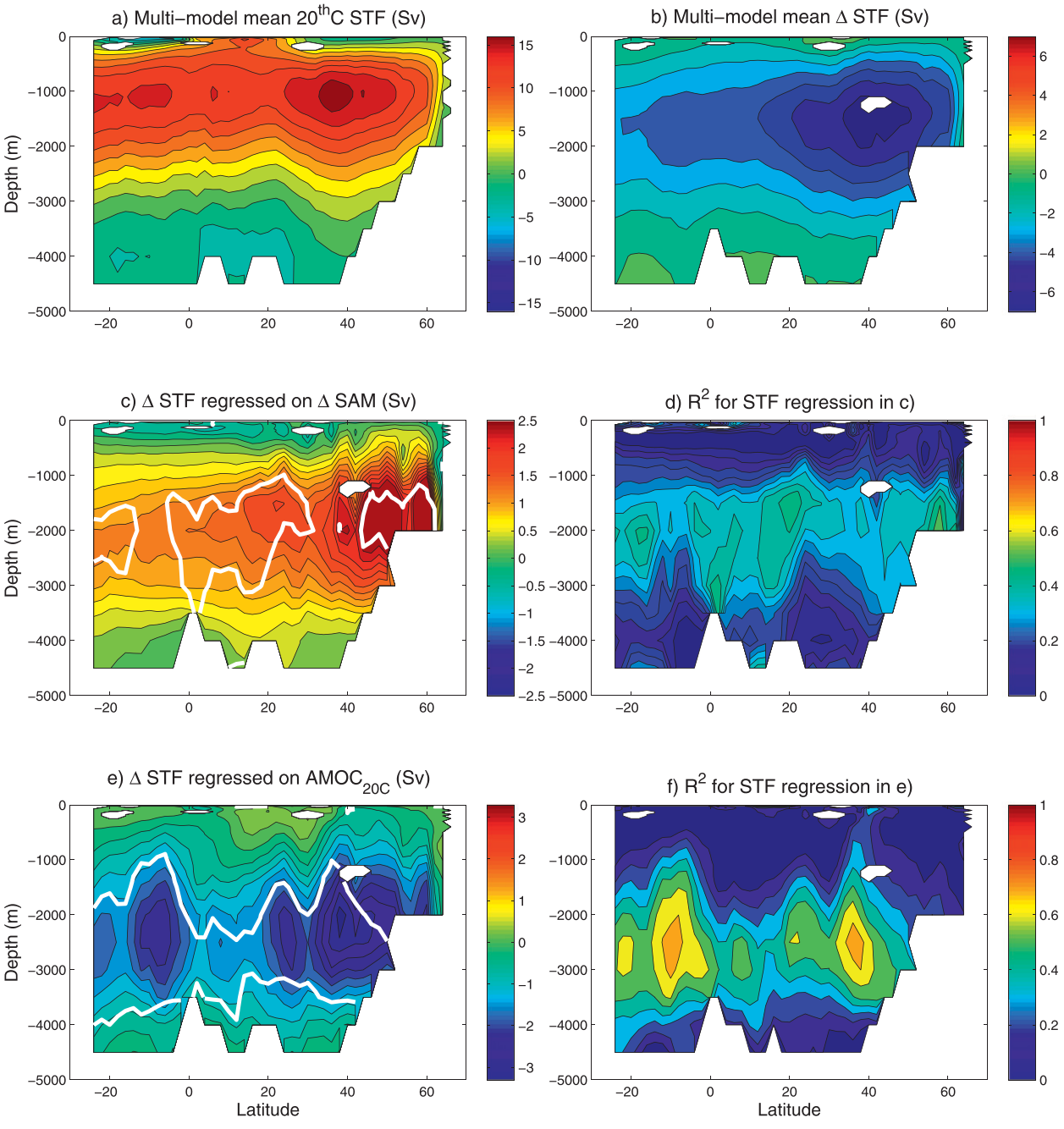

FIG. 2. (a) Multimodel mean AMOC streamfunction (STF) for the period 1960–99. (b) Multimodel mean AMOC streamfunction response from the period $1960–99_{mean}$ to the period $2060–99_{mean}$ (section 2). (c) Map of regression slopes B for the STF response regressed on the normalized SAM index response. B is consistently positive here, suggesting that models predicting the greatest increase in the SAM index also predict the lowest weakening of the AMOC. (d) Map of the R^2 statistic based on the regressions in (c). (e) Map of regression slopes B for the STF response regressed on the initial $1960–99_{mean}$ AMOC index. Models with the strongest initial AMOC also tend to show the greatest weakening of the AMOC. (f) Map of the R^2 statistic based on the regressions in (e). The areas bounded by white contours in (c),(e) indicate where the results are inconsistent with the null hypothesis at the 95% confidence level.

and Cruz 2009; de Boer et al. 2010; Marini et al. 2011). These studies all find some form of causality for the relationship between Southern Hemisphere winds and the AMOC—although the mechanisms are not all the same—and we investigate the possibilities below. Our results add to the evidence that wind forcing does indeed play an important role in the Atlantic overturning circulation, at least in coupled climate models. As far as we

are aware, this is the first study to show this relationship in a multimodel analysis and under greenhouse gas forcing.

b. Physical mechanisms

The studies given above suggest a variety of mechanisms via which the SAM may influence the AMOC. For simplicity, we separate these into three broad categories and investigate each one in the following sections.

Direct mechanical reinforcement of the AMOC by an increase in the SAM may be possible through increased northward Ekman transport out of the Southern Ocean and corresponding deepening of the Atlantic pycnocline (Gnanadesikan 1999; Klinger and Cruz 2009). This would be associated with increased upwelling around Antarctica, drawing water up from the depths of the deep-ocean ridges where the NADW resides—due to restraints on geostrophic flow in middepths—and closing the circulation loop (Toggweiler and Samuels 1995).

It is also possible that an increase in the SAM might result in an increase in the wind-driven salt advection into the Atlantic Ocean and a subsequent strengthening of the AMOC through farther northward advection of the salt (Marini et al. 2011; Sijp and England 2009).

The third potential linking mechanism is the influence of large-scale atmospheric teleconnections. The North Atlantic Oscillation (NAO) may have an effect on the strength of the AMOC through changes in the wind-driven surface ocean circulation and surface buoyancy fluxes at high latitudes (e.g., Dong and Sutton 2005; Mignot and Frankignoul 2005; Bellucci and Richards 2006; Deshayes and Frankignoul 2008). The NAO and the SAM might be expected to respond similarly to climate change, since temperature changes in the tropical troposphere and in the stratosphere are believed to be important in both responses (although more local temperature changes complicate matters). If they do and if they both influence the AMOC in the same way, it will be difficult to decipher which is the true driver. The SAM has also been implicated in tropical precipitation processes linked to increasing Atlantic salinity (Marini et al. 2011).

To establish which (if any) of these mechanisms are important, in the rest of this section we consider the mean climate change responses of a range of variables, as well as their regressions on the SAM response. We focus on the Southern and Atlantic Oceans.

1) Southern Ocean and South Atlantic mechanisms

Since the SAM is the leading mode of climate variability in the Southern Hemisphere, one might expect changes in the SAM index to be related to identifiable oceanic and atmospheric responses here. Some of these responses, such as Ekman transport, are implicated in the direct mechanical forcing mechanism described above.

The multimodel mean responses (2060–99 minus 1960–99) of six variables in the Southern Hemisphere are shown in Fig. 3. Figure 4 shows B for the regressions of these six variables on the SAM index. The maps of B show similar patterns and magnitudes (when scaled up by 1.56; see section 2b) to the mean response for every variable except salinity, suggesting that the mean response in the Southern Hemisphere is well described by the SAM. The increase in westerly wind strength between 40° and 70°S (Fig. 3a) is the dominant factor in the increase in the SAM index, with the increase in easterly wind strength between 20° and 40°S playing a slightly smaller role.

The calculated Ekman transport regressed on the increasing SAM index (Fig. 4c) shows the expected enhanced northward flow out of the Southern Ocean into the closed Atlantic basin. The R^2 values for the five remaining variables are somewhat inconsistent (not shown), but the patterns of B are consistent with increased upwelling south of 55°S. Decreases in sea surface temperature (Fig. 4f) and increases in salinity (Fig. 4e), despite increased precipitation minus evaporation ($P - E$) (Fig. 4d), all support this conclusion. The barotropic streamfunction (Fig. 4b) suggests that there is also a spin up of the Antarctic Circumpolar Current (ACC) and of the Southern Hemisphere subtropical gyres, again expected because of the increasing SAM. The gyres also shift poleward, with the notable result of increasing the salinity and sea surface temperature in the Agulhas region of the southern Indian Ocean. These changes are all consistent with those found by other authors (e.g., Hall and Visbeck 2002; Cai et al. 2005; Beal et al. 2011; Wang et al. 2011). The physically consistent response of each variable to an increased SAM suggests that parts of the mechanism neatly summarized by Gnanadesikan (1999) are indeed operating within these models. An increase in northward Ekman transport acts to generate upwelling in the Southern Ocean and an associated spin up of the ACC.

The increase in northward Ekman transport associated with the increase in the SAM index is around 1 Sv when summed across the southern boundary of the Atlantic basin. This is the same as the amount of water shown flowing northward above 2000 m at 20°S in Fig. 2c and suggests that much of the extra northward flow of the AMOC related to the SAM could be supplied by the Ekman transport because of increased Southern Ocean westerlies.

The magnitude of the AMOC response to a given wind forcing is consistent with values in the literature (e.g., Gnanadesikan 1999; Johnson et al. 2007; Klinger

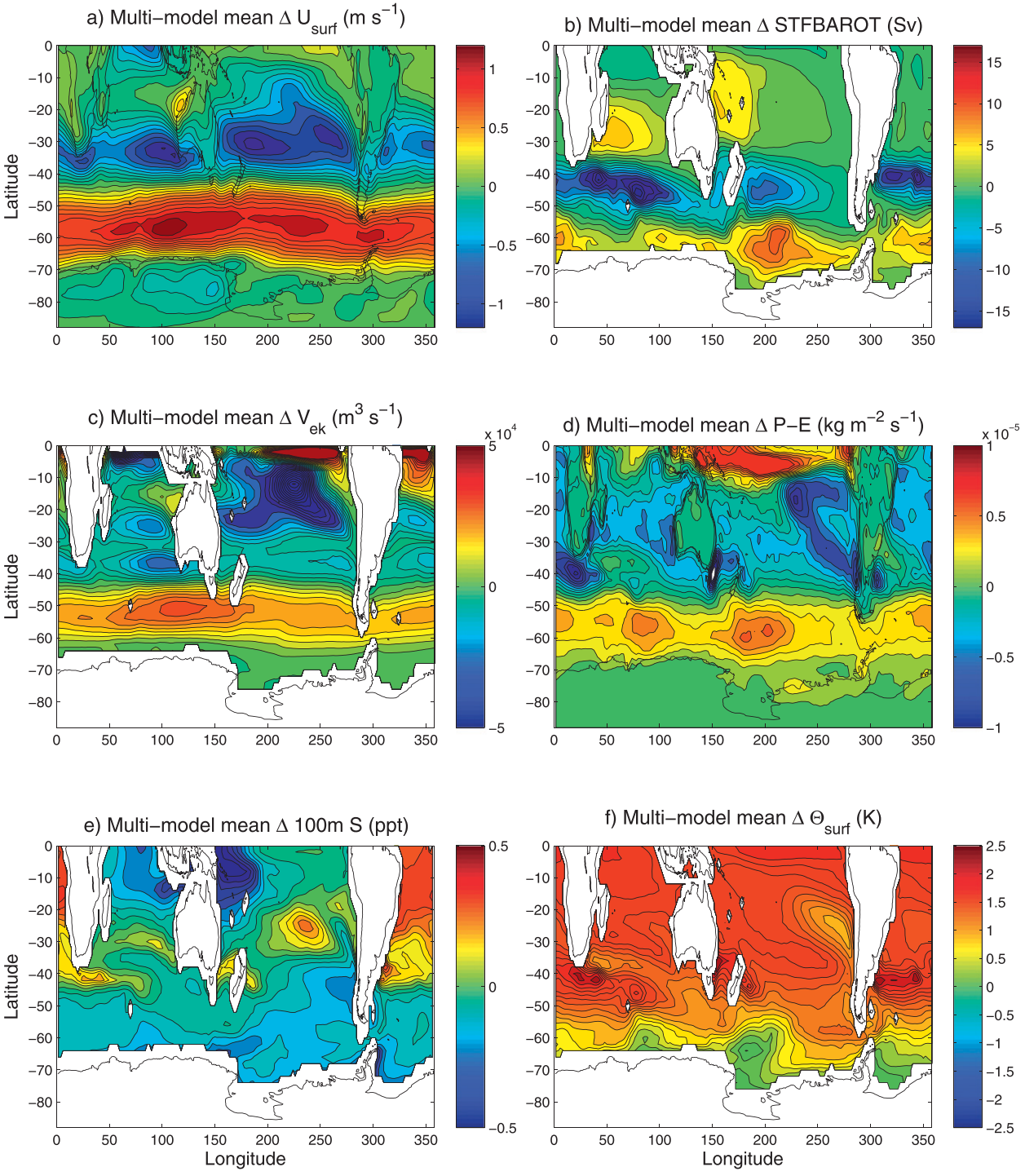

FIG. 3. Southern Hemisphere maps of the multimodel mean response (2060–99 minus 1960–99) of six variables: (a) zonal (westerly) surface wind speed U_{surf}, (b) barotropic streamfunction (STFBAROT), (c) northward Ekman transport per 2° latitude V_{ek}, (d) $P - E$, (e) salinity at 100m below the ocean surface S, and (f) sea surface temperature Θ_{surf}.

and Cruz 2009). This, along with the findings above, lends weight to the idea that it is the direct mechanical forcing of the Southern Ocean by winds that is the reason for the SAM–AMOC relationship seen in the CMIP3 models.

If this is the case, there should be some response in the vertical density structure of the Atlantic that is related to the SAM. The multimodel mean regions occupied by various water masses for the period 1960–99 are evident

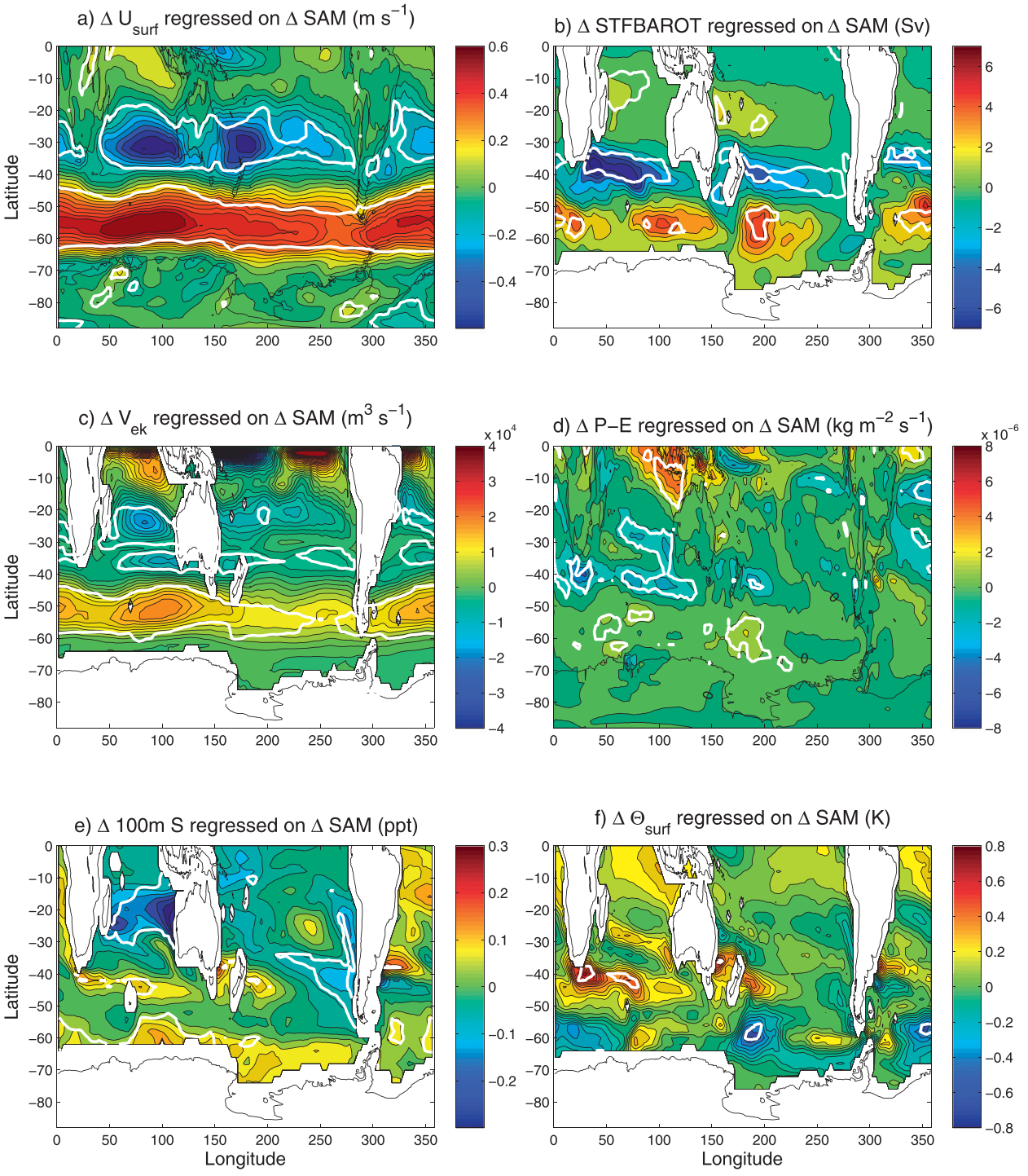

FIG. 4. Maps of best-fit regression line slopes (B) for regressions on the SAM index response in the Southern Hemisphere. The SAM index response has been normalized so that each map shows the pattern related to one standard deviation of the spread between the models: (a) zonal (westerly) surface wind speed U_{surf}. (b) STFBAROT, (c) northward Ekman transport per 2° latitude V_{ek}, (d) $P - E$, (e) salinity at 100 m below the ocean surface S, and (f) sea surface temperature Θ_{surf}. The areas bounded by white contours indicate where the results are inconsistent with the null hypothesis at the 95% confidence level.

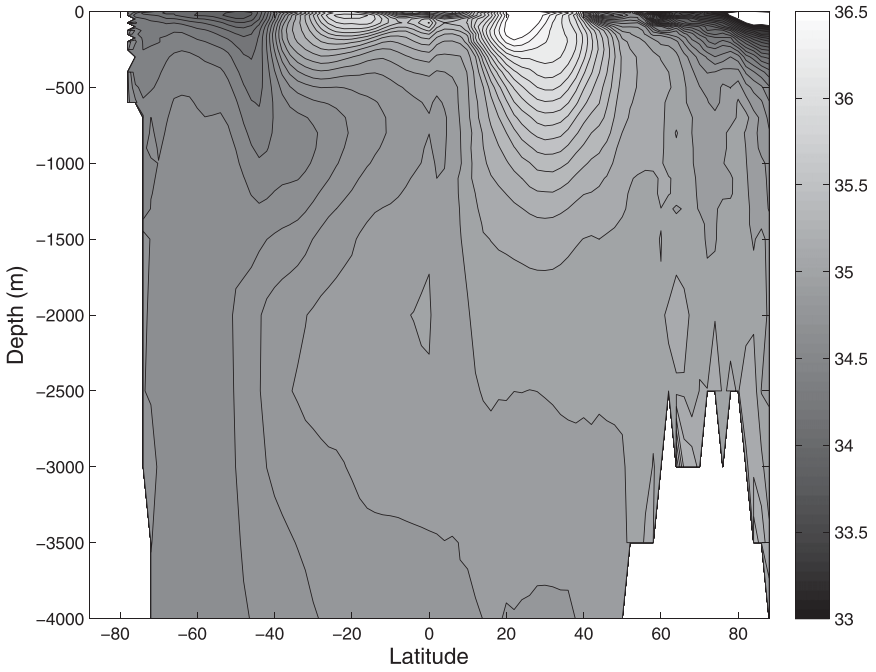

FIG. 5. Multimodel mean, zonally averaged Atlantic salinity for the period $1960–99_{mean}$, showing the three major water masses in the Atlantic Ocean.

from a plot of salinity (Fig. 5). The relatively saline water mass that fills much of the Atlantic basin is the NADW. The Antarctic Intermediate Water (AAIW) is the relatively freshwater mass, which can be up to 2000 m deep at 40°S and gets progressively shallower farther north. The Antarctic Bottom Water (AABW) has a weak, deep, and relatively fresh signature, although it is missing in several models.

The multimodel mean potential temperature Θ response (2060–99 minus 1960–99) shows an increase everywhere in the ocean (Fig. 6a). The salinity response (Fig. 6c) shows a predicted freshening of the NADW, due to the fresh surface water anomaly in the deep-water formation regions. The Northern Hemisphere subtropical gyre becomes saltier, although the major increase in salinity is at shallow depths. This suggests a shallowing of its depth of influence and a reduction in downwelling in the gyre. The temperature response dominates over salinity in determining the density response in much of the ocean (Fig. 6e); however, the freshening of the high-latitude North Atlantic is important.

Cross sections of the regression coefficient B for the same variables show that there is a cooling and freshening of a large mass of water between 2500 and 750 m associated with an increase in the SAM (Figs. 6b,d). This is significant and associated with high R^2 values for both variables. It is dominated by changes near the deep western boundary. This supports the idea that an increase in the SAM is associated with a deepening of the lower branch (NADW) of the AMOC, as suggested by its regression on the SAM (Fig. 2c). A deepening of the relatively saline NADW should result in changing salinity transport, resulting in enhanced salinity in the new path of the NADW and freshening above. It is unlikely that the change in properties is due to a consistent change in the location of deep-water formation, because this is very different in each model. These plots suggest that oceanic properties such as salinity and temperature are responding to the SAM-driven changes in the AMOC circulation, rather than forcing the circulation to change.

Despite the significant changes in Θ and salinity associated with the SAM, there is very little significant change in the associated density field (Fig. 6f). While this supports the conclusion above, it suggests that the pycnocline does not deepen in response to enhanced winds [as in Gnanadesikan (1999) and Klinger and Cruz (2009)]. However, the vertical resolution in this study is too low to detect changes in pycnocline depth corresponding to a 2.5-Sv change in maximum AMOC strength.

All of our findings so far have been consistent with direct mechanical forcing of the AMOC by the SAM through the Southern Ocean. Below, we explore the remaining two categories of mechanism that could link the SAM and the AMOC.

2) NORTHWARD SALT FLUX ACROSS 30°S

To test whether the salt flux into the Atlantic is affected by changes in the SAM, we calculate the change

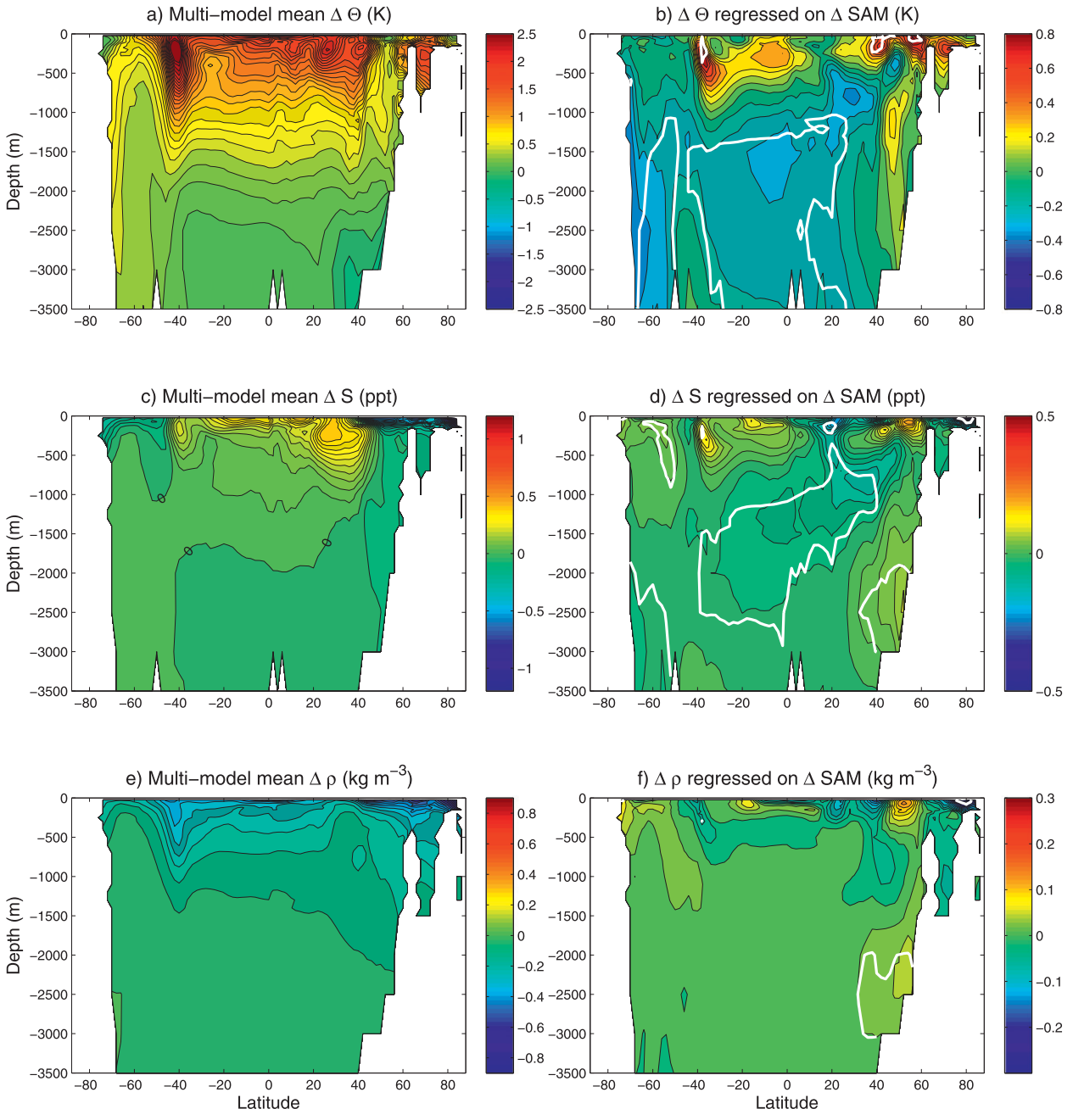

FIG. 6. Atlantic meridional cross sections of (a) multimodel mean response (2060–99 minus 1960–99) in potential temperature Θ. (b) best-fit regression line slopes B for the Θ response regressed on the SAM index response across model space, (c) multimodel salinity S response, (d) best-fit regression line slopes B for the S response regressed on the SAM index response across model space, (e) multimodel potential density ρ response, and (f) best-fit regression line slopes B for the ρ response regressed on the SAM index response across model space. The SAM index response has been normalized so that each map shows the pattern related to one standard deviation of the spread between the models. The areas bounded by white contours indicate where the results are inconsistent with the null hypothesis at the 95% confidence level.

in the northward salt transport across 30°S into the Atlantic basin for each model,

$$\Delta\text{salt transport} = \Delta \sum_{\text{longitude}} \sum_{\text{depth}} (Sv),$$

where S is salinity and v is meridional velocity. The responses are then regressed on both the SAM index and the change in the maximum AMOC streamfunction at 24°S (Fig. 7). The regressions show a positive relationship between changes in the northward salinity

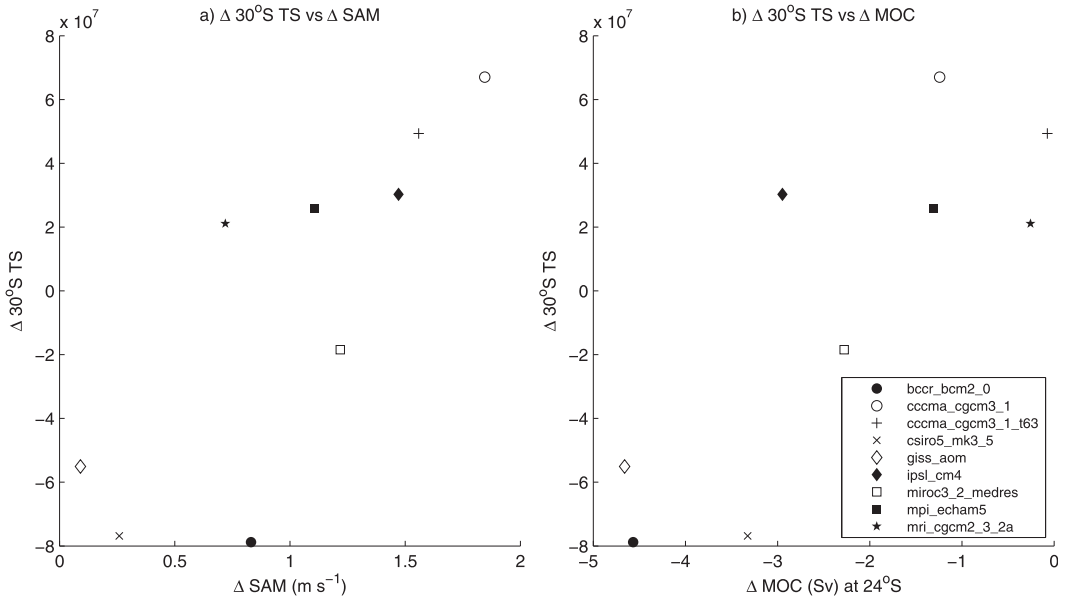

FIG. 7. Northward salt transport (TS) response at 30°S integrated over the depth and width of the Atlantic Ocean, plotted against (a) the SAM index response and (b) the change in the maximum AMOC streamfunction at 24°S (near to where the salt flux is calculated).

flux and these two indices. For the regression on the SAM index, $R^2 = 0.66$ and $p = 0.0075$; for the regression on the maximum AMOC streamfunction at 24°S, $R^2 = 0.67$ and $p = 0.0071$. It seems that the salt flux increase is likely to be a feedback on the original AMOC strengthening generated by the increasing SAM index. Once the SAM has begun to reinforce the AMOC, the ocean acts to advect more salt into the Atlantic, further stabilizing the overturning circulation. Changing properties of the Agulhas system (Fig. 4e,f) may also be involved, through increased salt leakage from the Indian Ocean into the Atlantic, although the effects of this are extremely difficult to quantify using our methodology.

3) NORTH ATLANTIC MECHANISMS

Figure 8 shows the multimodel mean response (2060–99 minus 1960–99) in the North Atlantic for the same six variables that were plotted in the Southern Hemisphere in Fig. 4. Zonal surface wind U_{surf} displays a north–south dipolar pattern (Fig. 8a) (also apparent in the Pacific), which has a similar pattern to the wind anomalies associated with a positive phase of the NAO (Hurrell and Deser 2009). The barotropic streamfunction response (Fig. 8b) indicates a northward shift and/or weakening of the subtropical gyre in the North Atlantic, potentially associated with the changes in the wind in Fig. 8a. This is consistent with the reduction of downwelling in the subtropical gyre suggested by Fig. 6c. The subpolar gyre response is much less clear. $P - E$ also shows the NAO-like dipolar pattern over both the Atlantic (Fig. 8d) and the Pacific and is therefore likely to be a result of intrinsic atmospheric processes. A broad freshening occurs at 100 m in depth in the area south of Greenland (Fig. 8e), presumably caused by the increase in $P - E$ there (e.g., Manabe et al. 1991). A tongue of fresh water that extends south along the African coast appears to be the result of the northern freshening being advected southward by the subtropical gyre. Sea surface temperature indicates a predicted warming of almost the entire ocean (Fig. 8f). The exception is in the high-latitude North Atlantic, where the warming is hampered because of the reduction of the AMOC circulation and its associated heat transport; this is a common result (Meehl et al. 2007; Drijfhout et al. 2012). The changes in sea surface temperature and salinity in the deep-water formation regions are thought to be the cause of the predicted reduction in AMOC strength (Dixon et al. 1999; Gregory et al. 2005).

Maps of the coefficient B for each variable regressed on the SAM index show different features to the mean responses (Fig. 9). Neither U_{surf} (Fig. 9a), Ekman transport (Fig. 9c), nor the barotropic streamfunction (Fig. 9b) show any clear pattern, and there is no significance at the 95% level for the majority of grid points. However, salinity shows a well-defined and significant pattern (Fig. 9e); a positive anomaly exists in the position of the subpolar gyre in the models, with a negative anomaly in the subtropics. The North Atlantic is the only region of the Northern Hemisphere where such high significance

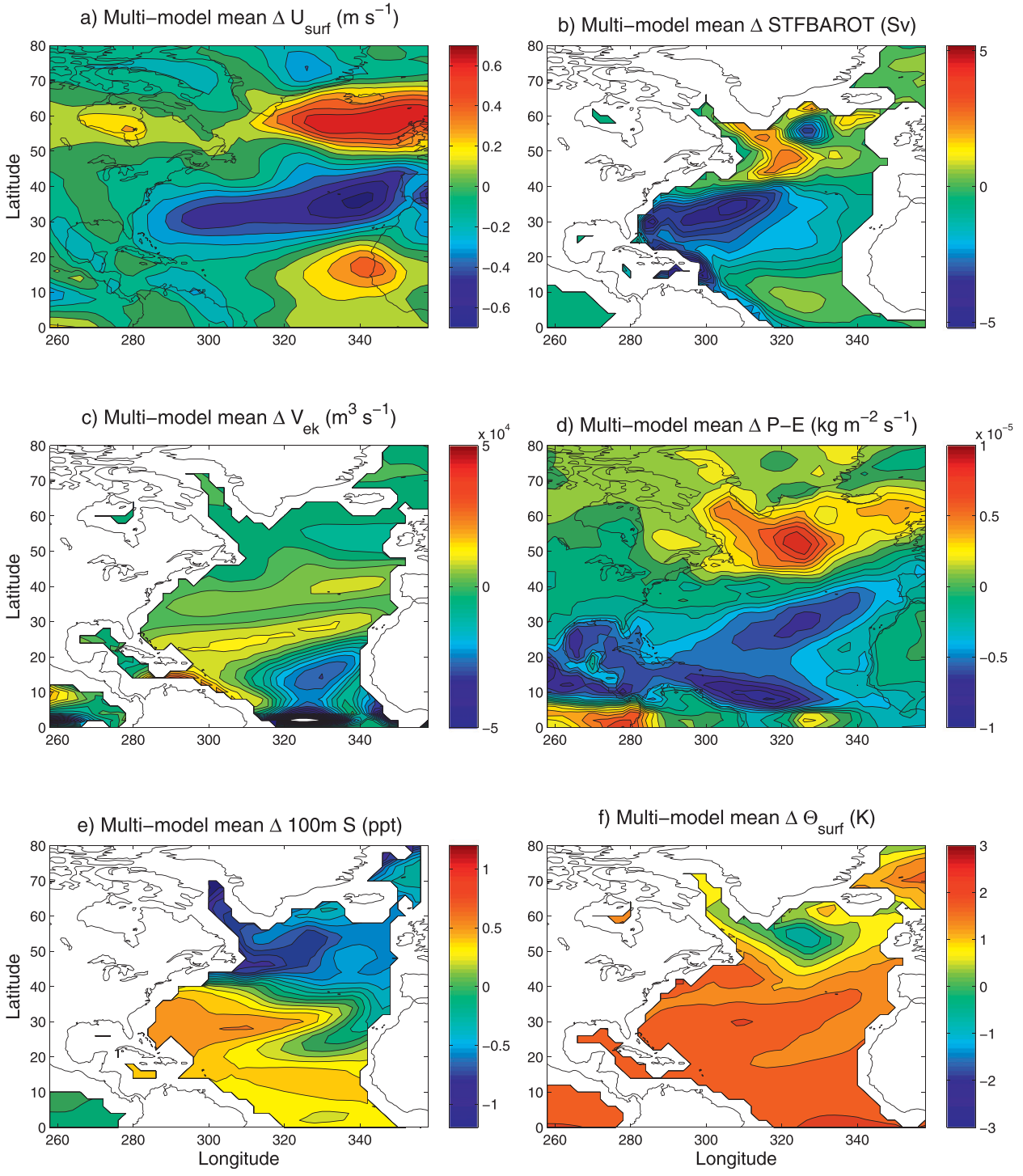

FIG. 8. Northern Hemisphere maps of the multimodel mean response (2060–99 minus 1960–99) of six variables: (a) zonal (westerly) surface wind speed U_{surf}, (b) STFBAROT, (c) northward Ekman transport per 2° latitude V_{ek}, (d) $P - E$, (e) salinity at 100 m below the ocean surface S, and (f) sea surface temperature Θ_{surf}.

is seen, suggesting that the results here are indeed important. High-latitude increases in salinity (Fig. 9e) and density (not shown) associated with an increase in the SAM are consistent with an increased AMOC. However, this relationship with the AMOC could be cause (since increasing density favors deep-water formation) or effect (since increasing the AMOC should lead to an increase in northward salt advection).

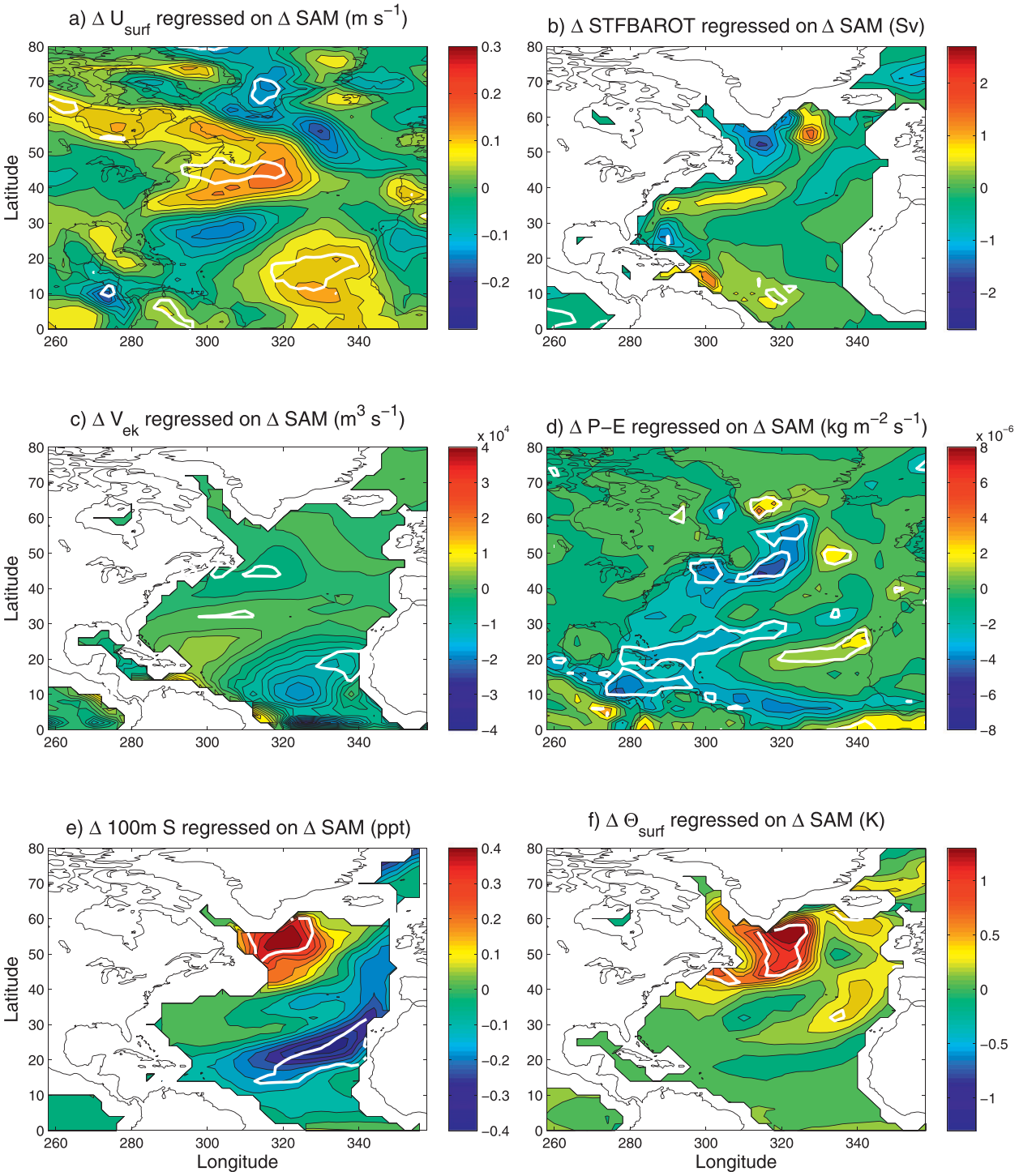

FIG. 9. Maps of best-fit regression line slopes B for regressions on the SAM index response in the Northern Hemisphere. The SAM index change has been normalized so that each map shows the pattern related to one standard deviation of the spread between the models: (a) zonal (westerly) surface wind speed U_{surf}, (b) STFBAROT, (c) northward Ekman transport per 2° latitude V_{ek}, (d) $P - E$, (e) salinity at 100 m below the ocean surface S, and (f) sea surface temperature Θ_{surf}. The areas bounded by white contours indicate where the results are inconsistent with the null hypothesis at the 95% confidence level.

We address this issue by looking at the maps of B for sea surface temperature and for $P - E$ (Figs. 9d,f). The patterns of these two variables and salinity are qualitatively similar, with a region of increased sea surface temperature, reduced $P - E$, and increased salinity over the subpolar gyre and a two-lobed pattern (where Θ_{surf} and salinity have opposite signs) extending south along the eastern boundary of the ocean. The simplest explanation for the similarity of these patterns is that the changes in sea surface temperature associated with the SAM are due to advection of warmer water from the south, which is also relatively salty. The temperature anomalies drive anomalies in $P - E$, which in turn reinforce the salinity anomalies.

While it is possible that these changes in ocean surface temperature are caused by atmospheric anomalies in the Northern Hemisphere linked to the SAM, this seems unlikely considering the lack of consistent pattern in B for U_{surf} regressed on the SAM response (Fig. 9a). It is more likely that the temperature changes are a result of increased advection of warm water into the subpolar gyre from the south due to the reinforcement of the AMOC. If this is the case, then the salinity anomalies in the high-latitude North Atlantic related to the increase in the SAM are another feedback process—like the salt advection at 30°S—that can further strengthen the AMOC, rather than a primary linking mechanism.

The lack of a clear North Atlantic surface wind response to the SAM also suggests that the SAM and NAO responses across the 11 models are unrelated. Values of $R^2 = 0.026$ and $p = 0.63$ for a regression of the NAO index response on the SAM index response show that this is indeed the case. The two indices do not evolve in a similar way in this set of models, and the SAM is much more strongly related to changes in the North Atlantic ocean than in the North Atlantic atmosphere, suggesting that the latter plays little role in the forcing of the AMOC by the SAM. Moreover, regressions of the AMOC response on the NAO index (not shown) are nowhere significant, suggesting that the NAO does not play as large a role as the SAM in modulating the strength of the AMOC under climate change in this set of models. Similarly, neither Fig. 4 nor Fig. 9 show significant links between the response of tropical variables and the SAM response, suggesting that the tropics do not link the SAM and the AMOC here, although other authors have found links between the SAM and tropical processes (e.g., Thompson and Lorenz 2004).

The absence of any clear interhemispheric, atmospheric response to the SAM suggests that the relationship between the SAM and the AMOC responses to greenhouse forcing stems primarily from the direct mechanical forcing of the AMOC by the SAM via Southern Ocean processes.

4. Discussion

a. *Note on the model subset and its relation to a wider range of models*

To assess whether our results are reproducible using more of the CMIP3 models, we have carried out a regression analysis of sea surface temperature for the 19 models where these data are available. The global pattern of the coefficient B for the sea surface temperature response regressed on the SAM index response is almost identical to that when using only 11 models (not shown). SAM-related cooling is observed around Antarctica, with increasing temperature in the Agulhas system and North Atlantic (the North Pacific shows a cooling). Values of p and R^2 are lower in the North Atlantic for this regression, but we argue that the similarity of the global pattern demonstrates that our results would be similar had more models been used in the analyses. It is also important to note that individual models used for the CMIP3 have been used in other studies (using alternative methods) where the SAM has been found to reinforce the AMOC (Delworth and Zeng 2008; Marini et al. 2011). Our study complements and extends these findings to a wider range of CMIP3 models.

We also consider the relevance of these results to the newer and larger set of models from phase 5 of CMIP (CMIP5), for which publications are beginning to emerge. They typically have better resolution than the CMIP3 models (Taylor et al. 2012), and all contain time-varying stratospheric ozone (Gillett and Fyfe 2013). However, their ocean components are still not eddy permitting and, despite the better representation of ozone changes, the SAM index still exhibits an increase in all seasons as the atmospheric greenhouse gas concentration increases (Gillett and Fyfe 2013). Like the CMIP3 models, the CMIP5 models all predict weakening of the AMOC (Cheng et al. 2013), and there is a poleward shift of the Southern Hemisphere subtropical gyres linked to the increasing SAM index (Meijers et al. 2012). These features of the CMIP5 model data suggest that they behave in very similar ways to the CMIP3 models, with some improvements with regards to ozone. We suggest that, if the same analyses were to be carried out on the CMIP5 models, the results would be similar to those obtained here.

b. *Drivers of spread in the SAM response*

To better understand the full set of processes operating here, it is useful to consider what may drive the spread in the SAM response between models.

First, it may be the case that models with greater sensitivity to greenhouse gas forcing display a greater response in the SAM index. The relationship between the SAM index response and the transient and equilibrium

climate sensitivities is positive as might be expected, but neither is significant (we find p values of $p = 0.27$ and $p = 0.30$ for regressions of the SAM index response on the transient and equilibrium climate sensitivities, respectively). This shows that differences in model SAM responses cannot be sufficiently explained by differences in climate sensitivity. Normalizing the responses of the climate variables by the global mean temperature change also has no significant impact on the results.

Second, we have found that in this set of models the SAM response is not obviously related to whether the models do or do not contain time-varying stratospheric ozone. Greenhouse gas emissions appear to be the dominant driver of changes in the SAM. However, this is inconsistent with other studies that have found that changes in ozone play an important role in observed and modeled changes in the SAM (Shindell and Schmidt 2004; Miller et al. 2006; Perlwitz et al. 2008; Son et al. 2009). This discrepancy is likely to be due to the exact subset of models used and the choice of time periods compared here.

It has been shown using a different subset of the CMIP3 climate models that the response of the SAM is related to its initial state (Kidston and Gerber 2010), although this was less clear in the austral summer months because of differences in model representation of the stratosphere. We carry out a similar test and find that, if the anomalous GISS-AOM is excluded, models with the weakest initial SAM show the biggest response, consistent with the above study. (The GISS-AOM has a very low initial SAM index and also displays the smallest response to climate forcing of any of the models, falling well outside the relationship defined by the other models.) This relationship is significant ($p = 0.035$), even though we are using the austral summer months. This suggests that, in general, the initial state of the SAM does indeed play a role in determining its response.

c. Eddy activity in the Southern Ocean

Because of the coarseness of the resolution of these CMIP3 climate models, they do not explicitly represent ocean eddies. Eddies are either parameterized using different versions of the Gent–McWilliams (GM) parameterization (Gent and McWilliams 1990; Visbeck et al. 1997) or are not represented at all. Of the set of models used here, CGCM3.1(T47), CGCM3.1(T63), CSIRO Mk3.0, MIROC3.2(medres), ECHAM/MPI-OM, and MRI-CGCM2.3.2 use constant GM coefficients; GFDL CM2.1 and IPSL-CM4 use varying but capped GM coefficients; BCCR-BCM2.0 is an isopycnal model that uses interface smoothing equivalent to a GM parameterization; and GISS-AOM and INM-CM3.0 do not contain eddy parameterization (Kuhlbrodt et al. 2012).

This presents a challenge for relating these results to the real ocean. Eddies extract energy from sloping density surfaces and act to flatten them (Lee et al. 1997). This means that in the Southern Ocean there is a time-varying bolus circulation that opposes the northward Ekman transport due to westerly winds. This has two implications for the climate change response of the Southern Ocean.

First, eddies may respond to changes in wind forcing by opposing changes in isopycnal slope, making the transport of the ACC relatively insensitive to wind forcing (e.g., Hallberg and Gnanadesikan 2006). Based on observational and modeling studies, it has been suggested that although the Antarctic Circumpolar Current (ACC) responds to changes in wind stress on short time scales (days to years) (Hughes et al. 2003; Meredith et al. 2004), it varies by a proportionally much smaller amount over longer time scales (Meredith et al. 2004; Meredith and Hogg 2006; Hogg et al. 2008; Böning et al. 2008; Munday et al. 2013). Such a phenomenon is known as eddy saturation.

Second, in an eddy-permitting model, the bolus circulation has been shown to increase as the strength of the westerly winds increases (Farneti and Delworth 2010). This counteracts the increased northward Ekman flow and therefore greatly reduces the effect of an increase in the westerly winds on the AMOC (eddy compensation).

Better agreement between models with eddy parameterization and those that are eddy permitting can be achieved if the GM coefficient is allowed to vary and the upper limit on the coefficient is removed (Farneti and Gent 2011; Gent and Danabasoglu 2011). However, in such models the GM coefficient is generally dependent on isopycnal slope and therefore, while the models may be eddy compensated, this requires a change in the isopycnal slope such that they cannot also be eddy saturated. The mean climate state of the models can be adversely affected (Farneti and Gent 2011). In any case, none of the models in this study have uncapped GM coefficients and are therefore unlikely to capture the full extent of eddy behavior under wind stress forcing.

There seems to be a growing consensus that the Southern Ocean is close to eddy saturated. If this is the case, then the effect of an increasing SAM on the ACC and on the AMOC in the twenty-first century may be rather limited. Although eddy compensation may not be so closely tied to eddy saturation as many authors assume (Meredith et al. 2012), its likely underestimation in these models has implications for their skill in predicting the AMOC response of the real ocean.

d. Are the predictions of the AMOC in climate models too conservative?

In the previous two sections, we have outlined two processes that are not well or consistently represented in

the CMIP3 models used for climate prediction: ozone recovery and ocean eddy activity. Both of these processes have a possible bearing on our results.

First, it has been shown in general that models with ozone recovery display weaker trends in the SAM in the twenty-first century (Miller et al. 2006; Perlwitz et al. 2008; Son et al. 2009), yet not all CMIP3 models include this. This may mean that the observed increasing trend in the SAM will not continue at such a rate if the effect of greenhouse gases is counteracted by ozone recovery in the future. If the SAM–AMOC relationship found here is representative of the wider range of models, this would mean that the CMIP3 climate models may be underestimating the full magnitude of AMOC decline. This hypothesis could be directly tested by analyzing the CMIP5 models, which all include time-varying ozone as discussed above.

Underestimation of AMOC weakening may be compounded by the effect of eddies in the real ocean, which may reduce the influence of the SAM on the AMOC through eddy compensation. If the magnitudes of the regression results obtained here are to be believed, the models may be underestimating the AMOC reduction by up to 1/3. This could have important implications for predicted ocean heat transport and both European and global climate, as well as potential implications for carbon cycling between the ocean and atmosphere. Note that the coarse resolution of the models may mean that other drivers of AMOC change are also misrepresented. Future studies should aim to better quantify the potential for and consequences of underestimation of the AMOC weakening in CMIP5 compared with higher-resolution models.

5. Summary

When subjected to greenhouse gas forcing, the southern annular mode (SAM) response of 11 climate models has been shown to reinforce the Atlantic meridional overturning circulation (AMOC) through the mechanisms of increased northward Ekman transport and upwelling in the Southern Ocean. These processes force a more vigorous AMOC, as well as increasing the salt flux across 30°S into the Atlantic. Once the AMOC has begun to respond to the Southern Hemisphere westerlies, a system of feedback processes is set in motion in the North Atlantic, involving warming of northern waters and associated evaporation and salinification. These processes increase the density of waters near the regions of deep-water formation, favoring deep convection and further AMOC reinforcement.

The overall effect of the increasing trend in the SAM is to reduce the predicted weakening of the AMOC by around 1/3. The intermodel spread in the SAM response can potentially explain up to 35% of the spread in AMOC responses, although this could be an overestimate. A large proportion of the spread in the response of the AMOC can also be explained by differences in its initial state. The same is true of the response in the SAM.

The effect of ocean eddies is likely underrepresented in the models investigated here, and this may mean that predictions of the weakening of the AMOC in these models are too conservative by up to 1/3. The lack of ozone recovery in some CMIP3 models may contribute to this effect. Further work is required on the nature of eddy compensation in the Southern Ocean to assess the skill of coarse resolution models and to investigate whether they underestimate the weakening of the AMOC or whether the SAM may indeed reduce the effects of climate change in the North Atlantic.

Acknowledgments. We thank Jonathan Gregory for supplying the script used for downloading the data and Anand Gnanadesikan for supplying some additional data. Also thanks to Peter Gent, Anand Gnanadesikan, and an anonymous reviewer for their constructive comments and to Jonathan Gregory, Lesley Allison, Till Kuhlbrodt, Nathan Gillett, and Agatha de Boer for discussion and feedback, which were extremely helpful. HLJ is supported by a Royal Society University Research Fellowship, and this project was funded by a Royal Society summer studentship.

REFERENCES

Alley, R. B., 2007: Wally was right: Predictive ability of the North Atlantic "conveyor belt" hypothesis for abrupt climate change. *Annu. Rev. Earth Planet. Sci.,* **35,** 241–272.

Beal, L. M., W. P. M. De Ruijter, A. Biastoch, and Z. Rainer, 2011: On the role of the agulhas system in ocean circulation and climate. *Nature,* **472,** 429–436.

Bellucci, A., and K. J. Richards, 2006: Effects of NAO variability on the North Atlantic Ocean circulation. *Geophys. Res. Lett.,* **33,** L02612, doi:10.1029/2005GL024890.

Böning, C. W., A. Dispert, M. Visbeck, S. R. Rintoul, and F. U. Schwarzkopf, 2008: The response of the Antarctic Circumpolar Current to recent climate change. *Nat. Geosci.,* **1,** 864–869.

Broecker, W. S., 1998: Paleocean circulation during the last deglaciation: A bipolar seesaw? *Paleoceanography,* **13,** 119–121.

——, G. H. Denton, R. L. Edwards, H. Cheng, R. B. Alley, and A. E. Putnam, 2010: Putting the younger dryas cold event into context. *Quat. Sci. Rev.,* **29** (9–10), 1078–1081.

Cai, W., G. Shi, T. Cowan, D. Bi, and J. Ribbe, 2005: The response of the southern annular mode, the East Australian Current, and the southern mid-latitude ocean circulation to global warming. *Geophys. Res. Lett.,* **32,** L23706, doi:10.1029/2005GL024701.

Cheng, W., J. C. H. Chiang, and D. Zhang, 2013: Atlantic meridional overturning circulation (AMOC) in CMIP5 models: RCP and historical simulations. *J. Climate,* **26,** 7187–7197.

Christensen, J. H., and Coauthors, 2007: Regional climate projections. *Climate Change 2007: The Physical Science Basis,* S. Solomon et al., Eds., Cambridge University Press, 847–940.

de Boer, A. M., and D. Nof, 2005: The island wind buoyancy connection. *Tellus,* **57,** 783–797.

——, J. R. Toggweiler, and D. M. Sigman, 2008: Atlantic dominance of the meridional overturning circulation. *J. Phys. Oceanogr.,* **38,** 435–450.

——, A. Gnanadesikan, N. R. Edwards, and A. J. Watson, 2010: Meridional density gradients do not control the Atlantic overturning circulation. *J. Phys. Oceanogr.,* **40,** 368–380.

Delworth, T. L., and F. Zeng, 2008: Simulated impact of altered Southern Hemisphere winds on the Atlantic meridional overturning circulation. *Geophys. Res. Lett.,* **35,** L20708, doi:10.1029/2008GL035166.

Deshayes, J., and C. Frankignoul, 2008: Simulated variability of the circulation in the North Atlantic from 1953 to 2003. *J. Climate,* **21,** 4919–4933.

Dixon, K. W., T. L. Delworth, M. J. Spelman, and R. J. Stouffer, 1999: The influence of transient surface fluxes on North Atlantic overturning in a coupled GCM climate change experiment. *Geophys. Res. Lett.,* **26,** 2749–2752.

Dong, B. W., and R. T. Sutton, 2005: Mechanism of interdecadal thermohaline circulation variability in a coupled ocean–atmosphere GCM. *J. Climate,* **18,** 1117–1135.

Drijfhout, S., G. J. van Oldenborgh, and A. Cimatoribus, 2012: Is a decline of AMOC causing the warming hole above the North Atlantic in observed and modeled warming patterns? *J. Climate,* **25,** 8373–8379.

Farneti, R., and T. L. Delworth, 2010: The role of mesoscale eddies in the remote oceanic response to altered Southern Hemisphere winds. *J. Phys. Oceanogr.,* **40,** 2348–2354.

——, and P. R. Gent, 2011: The effects of the eddy-induced advection coefficient in a coarse-resolution coupled climate model. *Ocean Modell.,* **39,** 135–145.

Flückiger, J., and Coauthors, 2004: N_2O and CH_4 variations during the last glacial epoch: Insight into global processes. *Global Biogeochem. Cycles,* **18,** GB1020, doi:10.1029/2003GB002122.

Fyfe, J. C., and O. A. Saenko, 2006: Simulated changes in the extratropical Southern Hemisphere winds and currents. *Geophys. Res. Lett.,* **33,** L06701, doi:10.1029/2005GL025332.

Gent, P. R., and J. C. McWilliams, 1990: Isopycnal mixing in ocean circulation models. *J. Phys. Oceanogr.,* **20,** 150–160.

——, and G. Danabasoglu, 2011: Response to increasing Southern Hemisphere winds in CCSM4. *J. Climate,* **24,** 4992–4998.

Gillett, N. P., and D. W. J. Thompson, 2003: Simulation of recent Southern Hemisphere climate change. *Science,* **302,** 273–275.

——, and J. C. Fyfe, 2013: Annular mode changes in the CMIP5 simulations. *Geophys. Res. Lett.,* **40,** 1189–1193, doi:10.1002/grl.50249.

Gnanadesikan, A., 1999: A simple predictive model for the structure of the oceanic pycnocline. *Science,* **283,** 2077–2079.

Gong, D. Y., and S. W. Wang, 1999: Definition of Antarctic Oscillation index. *Geophys. Res. Lett.,* **26,** 459–462.

Gregory, J. M., and Coauthors, 2005: A model intercomparison of changes in the Atlantic thermohaline circulation in response to increasing atmospheric CO_2 concentration. *Geophys. Res. Lett.,* **32,** L12703, doi:10.1029/2005GL023209.

Hall, A., and M. Visbeck, 2002: Synchronous variability in the Southern Hemisphere atmosphere, sea ice, and ocean resulting from the annular mode. *J. Climate,* **15,** 3043–3057.

——, and X. Qu, 2006: Using the current seasonal cycle to constrain snow albedo feedback in future climate change. *Geophys. Res. Lett.,* **33,** L03502, doi:10.1029/2005GL025127.

Hallberg, R., and A. Gnanadesikan, 2006: The role of eddies in determining the structure and response of the wind-driven Southern Hemisphere overturning: Results from the modeling eddies in the Southern Ocean (MESO) project. *J. Phys. Oceanogr.,* **36,** 2232–2252.

Hogg, A. M., M. P. Meredith, J. R. Blundell, and C. Wilson, 2008: Eddy heat flux in the Southern Ocean: Response to variable wind forcing. *J. Climate,* **21,** 608–620.

Hughes, C. W., P. L. Woodworth, M. P. Meredith, V. Stepanov, T. Whitworth, and A. R. Pyne, 2003: Coherence of Antarctic sea levels, Southern Hemisphere annular mode, and flow through Drake Passage. *Geophys. Res. Lett.,* **30,** 1464, doi:10.1029/2003GL017240.

Hurrell, J. W., and C. Deser, 2009: North Atlantic climate variability: The role of the North Atlantic Oscillation. *J. Mar. Syst.,* **78,** 28–41.

Johnson, H. L., D. P. Marshall, and D. A. J. Sproson, 2007: Reconciling theories of a mechanically driven meridional overturning circulation with thermohaline forcing and multiple equilibria. *Climate Dyn.,* **29** (7–8), 821–836.

Jones, J. M., and M. Widmann, 2004: Atmospheric science—Early peak in Antarctic Oscillation index. *Nature,* **432,** 290–291.

Kidston, J., and E. P. Gerber, 2010: Intermodel variability of the poleward shift of the austral jet stream in the CMIP3 integrations linked to biases in 20th century climatology. *Geophys. Res. Lett.,* **37,** L09708, doi:10.1029/2010GL042873.

Klinger, B. A., and C. Cruz, 2009: Decadal response of global circulation to Southern Ocean zonal wind stress perturbation. *J. Phys. Oceanogr.,* **39,** 1888–1904.

Knight, J. R., R. J. Allan, C. K. Folland, M. Vellinga, and M. E. Mann, 2005: A signature of persistent natural thermohaline circulation cycles in observed climate. *Geophys. Res. Lett.,* **32,** L20708, doi:10.1029/2005GL024233.

Kuhlbrodt, T., A. Griesel, M. Montoya, A. Levermann, M. Hofmann, and S. Rahmstorf, 2007: On the driving processes of the Atlantic meridional overturning circulation. *Rev. Geophys.,* **45,** RG2001, doi:10.1029/2004RG000166.

——, R. S. Smith, Z. Wang, and J. M. Gregory, 2012: The influence of eddy parameterizations on the transport of the Antarctic Circumpolar Current in coupled climate models. *Ocean Modell.,* **52,** 1–8.

Lee, M. M., D. P. Marshall, and R. G. Williams, 1997: On the eddy transfer of tracers: Advective or diffusive? *J. Mar. Res.,* **55,** 483–505.

Manabe, S., R. J. Stouffer, M. J. Spelman, and K. Bryan, 1991: Transient responses of a coupled ocean atmosphere model to gradual changes of atmospheric CO_2. Part I: Annual mean response. *J. Climate,* **4,** 785–818.

Marini, C., C. Frankignoul, and J. Mignot, 2011: Links between the southern annular mode and the Atlantic meridional overturning circulation in a climate model. *J. Climate,* **24,** 624–640.

Marshall, G. J., 2003: Trends in the southern annular mode from observations and reanalyses. *J. Climate,* **16,** 4134–4143.

——, P. A. Stott, J. Turner, W. M. Connolley, J. C. King, and T. A. Lachlan-Cope, 2004: Causes of exceptional atmospheric circulation changes in the Southern Hemisphere. *Geophys. Res. Lett.,* **31,** L14205, doi:10.1029/2004GL019952.

McManus, J. F., R. Francois, J. M. Gherardi, L. D. Keigwin, and S. Brown-Leger, 2004: Collapse and rapid resumption of Atlantic meridional circulation linked to deglacial climate changes. *Nature,* **428,** 834–837.

Meehl, G. A., and Coauthors, 2007: Global climate projections. *Climate Change 2007: The Physical Science Basis,* S. Solomon et al., Eds., Cambridge University Press, 747–845.

Meijers, A. J. S., E. Shuckburgh, N. Bruneau, J.-B. Sallee, T. J. Bracegirdle, and Z. Wang, 2012: Representation of the Antarctic Circumpolar Current in the CMIP5 climate models and future changes under warming scenarios. *J. Geophys. Res.,* **117,** C12008, doi:10.1029/2012JC008412.

Meredith, M. P., and A. M. Hogg, 2006: Circumpolar response of Southern Ocean eddy activity to a change in the southern annular mode. *Geophys. Res. Lett.,* **33,** L16608, doi:10.1029/2006GL026499.

——, P. L. Woodworth, C. W. Hughes, and V. Stepanov, 2004: Changes in the ocean transport through Drake Passage during the 1980s and 1990s, forced by changes in the southern annular mode. *Geophys. Res. Lett.,* **31,** L21305, doi:10.1029/2004GL021169.

——, A. C. N. Garabato, A. M. Hogg, and R. Farneti, 2012: Sensitivity of the overturning circulation in the Southern Ocean to decadal changes in wind forcing. *J. Climate,* **25,** 99–110.

Mignot, J., and C. Frankignoul, 2005: The variability of the Atlantic meridional overturning circulation, the North Atlantic Oscillation, and the El Niño–Southern Oscillation in the Bergen Climate Model. *J. Climate,* **18,** 2361–2375.

Mikolajewicz, U., and R. Voss, 2000: The role of the individual air-sea flux components in CO_2-induced changes of the ocean's circulation and climate. *Climate Dyn.,* **16,** 627–642.

Miller, R. L., G. A. Schmidt, and D. T. Shindell, 2006: Forced annular variations in the 20th century Intergovernmental Panel on Climate Change Fourth Assessment Report models. *J. Geophys. Res.,* **111,** D18101, doi:10.1029/2005JD006323.

Munday, D. R., H. L. Johnson, and D. P. Marshall, 2013: Eddy saturation of equilibriated circumpolar currents. *J. Phys. Oceanogr.,* **43,** 507–532.

Obata, A., 2007: Climate–carbon cycle model response to freshwater discharge into the North Atlantic. *J. Climate,* **20,** 5962–5976.

Pennell, C., and T. Reichler, 2011: On the effective number of climate models. *J. Climate,* **24,** 2358–2367.

Perlwitz, J., S. Pawson, R. L. Fogt, J. E. Nielsen, and W. D. Neff, 2008: Impact of stratospheric ozone hole recovery on Antarctic climate. *Geophys. Res. Lett.,* **35,** L08714, doi:10.1029/2008GL033317.

Robinson, L. F., J. F. Adkins, L. D. Keigwin, J. Southon, D. P. Fernandez, S. L. Wang, and D. S. Scheirer, 2005: Radiocarbon variability in the western North Atlantic during the last deglaciation. *Science,* **310,** 1469–1473.

Schmittner, A., 2005: Decline of the marine ecosystem caused by a reduction in the Atlantic overturning circulation. *Nature,* **434,** 628–633.

Seager, R., and D. S. Battisti, 2007: Challenges to our understanding of the general circulation: Abrupt climate change. *Global Circulation of the Atmosphere,* T. Schneider and A. H. Sobel, Eds., Princeton University Press, 332–372.

Shindell, D. T., and G. A. Schmidt, 2004: Southern Hemisphere climate response to ozone changes and greenhouse gas increases. *Geophys. Res. Lett.,* **31,** L18209, doi:10.1029/2004GL020724.

Sijp, W. P., and M. H. England, 2009: Southern Hemisphere westerly wind control over the ocean's thermohaline circulation. *J. Climate,* **22,** 1277–1286.

Solomon, S., D. Qin, M. Manning, Z. Chen, M. Marquis, K. B. Averyt, M. Tignor, and H. L. Miller, Eds., 2007: *Climate Change 2007: The Physical Science Basis.* Cambridge University Press, 996 pp.

Son, S. W., and Coauthors, 2008: The impact of stratospheric ozone recovery on the Southern Hemisphere westerly jet. *Science,* **320,** 1486–1489.

——, N. F. Tandon, L. M. Polvani, and D. W. Waugh, 2009: Ozone hole and Southern Hemisphere climate change. *Geophys. Res. Lett.,* **36,** L15705, doi:10.1029/2009GL038671.

Sowers, T., 2006: Late quaternary atmospheric CH_4 isotope record suggests marine clathrates are stable. *Science,* **311,** 838–840.

Taylor, K. E., R. J. Stouffer, and G. A. Meehl, 2012: An overview of CMIP5 and the experiment design. *Bull. Amer. Meteor. Soc.,* **93,** 485–498.

Thompson, D. W. J., and J. M. Wallace, 2000: Annular modes in the extratropical circulation. Part I: Month-to-month variability. *J. Climate,* **13,** 1000–1016.

——, and S. Solomon, 2002: Interpretation of recent Southern Hemisphere climate change. *Science,* **296,** 895–899.

——, and D. J. Lorenz, 2004: The signature of the annular modes in the tropical troposphere. *J. Climate,* **17,** 4330–4342.

Thorpe, R. B., J. M. Gregory, T. C. Johns, R. A. Wood, and J. F. B. Mitchell, 2001: Mechanisms determining the Atlantic thermohaline circulation response to greenhouse gas forcing in a non-flux-adjusted coupled climate model. *J. Climate,* **14,** 3102–3116.

Toggweiler, J. R., and B. Samuels, 1995: Effect of Drake Passage on the global thermohaline circulation. *Deep-Sea Res. I,* **42,** 477–500.

——, and J. Russell, 2008: Ocean circulation in a warming climate. *Nature,* **451,** 286–288.

Vellinga, M., and R. A. Wood, 2002: Global climatic impacts of a collapse of the Atlantic thermohaline circulation. *Climatic Change,* **54,** 251–267.

Visbeck, M., J. Marshall, T. Haine, and M. Spall, 1997: Specification of eddy transfer coefficients in coarse-resolution ocean circulation models. *J. Phys. Oceanogr.,* **27,** 381–402.

Wang, Y. J., H. Cheng, R. L. Edwards, Z. S. An, J. Y. Wu, C. C. Shen, and J. A. Dorale, 2001: A high-resolution absolute-dated late pleistocene monsoon record from Hulu Cave, China. *Science,* **294,** 2345–2348.

Wang, Z., T. Kuhlbrodt, and M. P. Meredith, 2011: On the response of the Antarctic Circumpolar Current transport to climate change in coupled climate models. *J. Geophys. Res.,* **116,** C08011, doi:10.1029/2010JC006757.

Wolfe, C. L., and P. Cessi, 2011: The adiabatic pole-to-pole overturning circulation. *J. Phys. Oceanogr.,* **41,** 1795–1810.

Wolff, E. W., J. Chappellaz, T. Blunier, S. O. Rasmussen, and A. Svensson, 2010: Millennial-scale variability during the last glacial: The ice core record. *Quat. Sci. Rev.,* **29** (21–22), 2828–2838.

Woollings, T., J. M. Gregory, J. G. Pinto, M. Reyers, and D. J. Brayshaw, 2012: Response of the North Atlantic storm track to climate change shaped by ocean-atmosphere coupling. *Nat. Geosci.,* **5,** 313–317.

Wunsch, C., 2002: What is the thermohaline circulation? *Science,* **298,** 1179–1181.

Yin, J. H., 2005: A consistent poleward shift of the storm tracks in simulations of 21st century climate. *Geophys. Res. Lett.,* **32,** L18701, doi:10.1029/2005GL023684.

Zickfeld, K., M. Eby, and A. J. Weaver, 2008: Carbon-cycle feedbacks of changes in the Atlantic meridional overturning circulation under future atmospheric CO_2. *Global Biogeochem. Cycles,* **22,** GB3024, doi:10.1029/2007GB003118.